HHS Public Access

Author manuscript

Neuropharmacology. Author manuscript; available in PMC 2018 September 01.

Published in final edited form as:

Neuropharmacology. 2017 September 01; 123: 46–54. doi:10.1016/j.neuropharm.2017.05.014.

Alcohol induces input-specific aberrant synaptic plasticity in the rat dorsomedial striatum

Tengfei Ma, **Britton Barbee**, **Xuehua Wang**, and **Jun Wang***

Department of Neuroscience and Experimental Therapeutics, College of Medicine, Texas A&M Health Science Center, Bryan, Texas

Abstract

Accumulated evidence suggests that the dorsomedial striatum (DMS) of the basal ganglia plays an essential role in pathological excessive alcohol consumption. The DMS receives multiple glutamatergic inputs. However, whether and how alcohol consumption distinctly affects these excitatory afferents to the DMS remains unknown. Here, we used optogenetics to selectively activate the rat medial prefrontal cortex (mPFC) and basolateral amygdala (BLA) inputs in DMS slices, and measured the effects of alcohol consumption on glutamatergic transmission in these corticostriatal and amygdalostriatal circuits. We found that excessive alcohol consumption increased AMPA receptor- and NMDA receptor (NMDAR)-mediated neurotransmission, as well as the GluN2B/NMDAR ratio, at the corticostriatal input to the DMS. The probability of glutamate release was increased selectively at the amygdalostriatal input. Interestingly, we discovered that paired activation of the mPFC and BLA inputs using dual-channel optogenetics induced robust long-term potentiation (LTP) of the corticostriatal input to the DMS. Taken together, these results indicate that excessive alcohol consumption potentiates glutamatergic transmission via a postsynaptic mechanism for the corticostriatal input and via a presynaptic mechanism for the amygdalostriatal input. These changes may in turn contribute to pathological alcohol consumption.

Keywords

Ethanol; medial prefrontal cortex; basolateral amygdala; dorsomedial striatum; glutamatergic receptor; optogenetics

1. Introduction

Repeated exposure to addictive drugs or alcohol induces aberrant synaptic plasticity, which is thought to contribute to the reinforcing properties of these compounds, and therefore to the development of addiction (Koob and Volkow, 2010; Luscher and Malenka, 2011). Drug-

*To whom correspondence should be addressed: Jun Wang, M.D., Ph.D., Department of Neuroscience and Experimental Therapeutics, College of Medicine, Texas A&M University Health Science Center, 2106 Medical Research and Education Building, 8447 Riverside Pkwy, Bryan, Texas 77807-3206, USA, Tel: +1 979-436-0389, Fax: +1 979-436-0086, jwang@medicine.tamhsc.edu.

induced synaptic plasticity has been reported in many brain regions, including the midbrain and the striatum (Koob and Volkow, 2010; Luscher and Malenka, 2011). The dorsomedial striatum (DMS), a brain region essential for goal-directed behaviors (Lovinger, 2010; Yin and Knowlton, 2006) that has been strongly implicated in drug and alcohol addiction, exhibits drug-evoked synaptic plasticity (Cheng et al, 2016; Corbit et al, 2014; Wang et al., 2012; Wang et al., 2015; Wang et al., 2010). For instance, excessive alcohol intake was shown to increase AMPA receptor (AMPAR) and NMD A receptor (NMDAR) activity in this area (Cheng et al, 2016; Wang et al, 2015; Wang et al., 2010).

Drug-evoked synaptic plasticity has been reported to be afferent input-specific (Britt et al, 2012; MacAskill et al, 2014; Pascoli et al., 2014; Seif et al, 2013). For instance, cocaine administration increases ventral striatal AMPAR activity at synapses receiving inputs from the medial prefrontal cortex (mPFC), but not at those receiving inputs from the basolateral amygdala (BLA) (Pascoli et al, 2014). Similarly, the DMS also receives inputs from the mPFC and the BLA (Corbit et al., 2013; Kupferschmidt et al, 2015). Importantly, both the corticostriatal (mPFC→DMS) and amygdalostriatal (BLA→DMS) pathways are critical for goal-directed behaviors, which are strongly modified by drug and alcohol intake (Balleine and O'Doherty, 2010; Corbit et al., 2013; Gerdeman et al, 2003). However, it is unclear whether alcohol consumption alters DMS glutamatergic transmission arising from the mPFC or BLA. It is also unknown whether the mPFC and BLA inputs both project to the same DMS neurons.

In this study, we used optogenetics to selectively activate the mPFC or BLA inputs to the DMS in alcohol-drinking and water control rats. We found that both inputs targeted the same DMS neurons. In addition, we discovered that excessive alcohol intake increased glutamatergic transmission elicited by the mPFC input, and stimulated glutamate release from the BLA afferent. Importantly, paired activation of the mPFC and BLA inputs induced long-term potentiation (LTP) of the mPFC input. These results indicate that excessive alcohol intake causes input-specific alterations, which may, in turn, contribute to pathological alcohol consumption.

2. Materials and methods

2.1 Reagents

Viral vectors (adeno-associated virus [AAV]-channelrhodopsin 2 [ChR2]-tdTomato, AAV-Chronos-green fluorescent protein [GFP], and AAV-Chrimson-tdTomato) were purchased from the University of North Carolina (Vector Core Facility). Ro 25–6981, 2,3-dihydroxy-6-nitro-7-sulfamoyl-benzo[f]quinoxaline-2,3-dione (NBQX), and (2R)-amino-5-phosphonovaleric acid; (2R)-amino-5-phosphonopentanoate (APV) were obtained from Tocris. All other reagents were purchased from Sigma.

2.2 Animals

Male Long-Evans rats (3–6 months-old) were used. All animals were kept in a temperature and humidity-controlled environment with a light:dark cycle of 12 h (lights on at 7:00 A.M.), with food and water available *ad libitum*. All animal procedures were approved by

the Texas A&M Institutional Animal Care and Use Committee and were conducted in agreement with the Guide for the Care and Use of Laboratory Animals, National Research Council, 1996.

2.3 Stereotaxic infusion

Animals were anesthetized with 3–4 % (vol/vol) isoflurane at 1.0 L/min and placed on a heating pad to maintain their body temperature. The head was leveled and craniotomies were performed using stereotaxic coordinates adapted from the rat brain atlas (Paxinos and Watson, 2007) (mPFC: AP1 3.2, ML1 0.65, DV1 −4.0; AP2 2.6, ML2 0.65, DV2 −4.0 from the Bregma. BLA: AP1 −2.1, ML1 4.5 DV1 9.0; AP2 −2.8, ML2 4.95, DV2 9.0 from the Bregma). The indicated viral vector (0.8–1 μL; AAV-ChR2 in Figures 2–5, AAV-Chronos-GFP and AAV-Chrimson-tdTomato in Figures 1 and 6) was bilaterally infused at each location at a rate of 0.08 μL/min. The injectors were left in place for an additional 5–10 min before removal. The scalp incision was then sutured, and the animals were returned to their home cage for ~6 weeks prior to electrophysiology recording.

2.4 Intermittent-access to 20% alcohol 2-bottle-choice drinking procedure

The procedure has been described previously (Wang et al., 2012; Wang et al., 2010). Rats were given access to one bottle of 20% alcohol (vol/vol) and one bottle of water for three 24-hour-sessions per week (Mondays, Wednesdays, and Fridays). On the Monday following the end of the housing acclimatization period, each rat was given access to 1 bottle of 20% alcohol and 1 bottle of water. After 24 hours, the alcohol bottle was replaced with a second water bottle that was available for the next 24 hours. This pattern was repeated on Wednesdays and Fridays. The rats had unlimited access to two bottles of water between the ethanol-access periods. The placement of the alcohol bottle was alternated each ethanol drinking session to control for side preference.

2.5 DMS slice preparation

This was conducted as described previously (Cheng et al., 2016; Wang et al., 2015). Briefly, coronal sections of the striatum (250 μm) were cut in an ice-cold solution containing (in mM): 40 NaCl, 143.5 sucrose, 4 KCl, 1.25 NaH_2PO_4, 26 $NaHCO_3$, 0.5 $CaCl_2$, 7 $MgCl_2$, 10 glucose, 1 sodium ascorbate, and 3 sodium pyruvate, saturated with 95% O_2 and 5% CO_2. Slices were then incubated in a 1:1 mixture of cutting solution and external solution at 32°C for 45 min. The external solution was composed of the following (in mM): 125 NaCl, 2.5 KCl, 2.0 $CaCl_2$, 1.0 $MgCl_2$, 1.25 NaH_2PO_4, 25 $NaHCO_3$, and 10 glucose, saturated with 95% O_2 and 5% CO_2. Slices were then maintained in external solution at room temperature until use.

2.6 Whole-cell patch-clamp recording

Slices were placed in a recording chamber and perfused with the external solution at a flow rate of 2 mL/min. Fluorescent axonal fibers were visualized using an epifluorescent microscope (Examiner A1, Zeiss). Neurons within the fluorescent area were selected for recording; stimulating electrodes were positioned ~150 μm away from the recording pipette. For selective stimulation of corticostriatal and amygdalostriatal inputs, 2-ms light was

delivered through the objective lens. We used 405-nm light to excite Chronos-expressing corticostriatal fibers and 590-nm light to stimulate Chrimson-containing amygdalostriatal inputs in the same recording (Figures 1 and 6). In other experiments (Figures 2–5), we used 470-nm light to excite ChR2-containing corticostriatal or amygdalostriatal afferents. Picrotoxin (100 μM) was included in the external solution to block $GABA_A$ receptor-mediated transmission. The patch pipettes contained (in mM): 119 CsMeSO4, 8 TEA.Cl, 15 HEPES, 0.6 EGTA, 0.3 Na3GTP, 4 MgATP, 5 QX-314, 7 phosphocreatine, with an osmolarity of ~280 mOsm/L. The pH was adjusted to 7.3 with KOH. Neurons were clamped at −70 mV unless stated otherwise. The input-output relationships for AMPAR- and NMDAR-mediated excitatory postsynaptic currents (EPSCs) were measured at 5 different stimulating laser powers. NMDAR-EPSCs were measured in the presence of 0.05 mM Mg^{2+} and NBQX (10 μM) to ensure that we could compare current data to previous studies in the same brain regions (Cheng et al, 2016; Wang et al, 2007; Wang et al., 2010). The proportion of NMDARs containing the GluN2B subunit (GluN2B/NMDAR ratio) was measured using the GluN2B antagonist, Ro 25–6981 (0.5 μM) (Cheng et al; Wang et al, 2010). GluN2B–EPSCs were obtained by digital subtraction of NMDAR-EPSCs in the presence of Ro 25–6981 from those EPSCs in the absence of this chemical. The GluN2B/NMDAR ratio was determined by the peak amplitude of GluN2B–EPSCs divided by the peak amplitude of NMDAR-EPSCs. While larger paired-pulse ratios (PPRs) of AMPAR-EPSCs were obtained using two electrical stimuli at an interval of 50 ms (Ding et al., 2008), we utilized an interval of 100 ms because ChR2 cannot reliably follow 20-Hz (equivalent to 50-ms intervals) light stimulation (Wu et al., 2015). The 100-ms interval was used for both electrical and optical stimulation so that we could compare these data. Electrical stimulation and optical stimulation were delivered alternately during some experiments (Figs. 2–5). A total of 52 rats were used to compare the difference between water (~1.58 neurons/rat) and alcohol (~1.53 neurons/rat) groups in Figures 2–5.

2.7 Field recording and LTP induction

Optogenetically-evoked field excitatory postsynaptic potentials/population spikes (fEPSP/PS) from the mPFC afferent were measured at 0.05 Hz in DMS slices. After a stable baseline was established, both the mPFC and BLA inputs were stimulated by 4 trains of stimuli (50 Hz ´ 2 sec), repeated at a 20-sec interval. fEPSP/PS were continuously measured for another 40 min. For the LT P analysis, the peak amplitude of each fEPSP/PS was measured and normalized to the mean peak amplitude of all fEPSP/PS during the 10-min baseline (Wang et al., 2012; Wang et al., 2004). The magnitude of fEPSP/PS potentiation was calculated by the mean peak amplitude of responses 30–40 min post-LTP induction.

2.8 Histology

Rats were intracardially perfused with 4% paraformaldehyde in phosphate-buffered saline. The brains were removed and post-fixed overnight in 4% paraformaldehyde at 4°C prior to dehydration in a 30% sucrose solution. To confirm viral vector infusion, the brains were cut into 50-μm coronal sections using a cryostat. Sections were imaged by a confocal scanning microscope (Olympus, FluoView 1200) using laser excitation at 473 nm for GFP and 559 nm for tdTomato.

2.9 Statistical analysis

Data obtained from 68 rats was included for analysis. All data are expressed as the mean ± the standard error of the mean. Data were analyzed by two-tailed *t* test (unpaired or paired), or by two-way analysis of variance with repeated measures (two-way RM ANOVA), followed by the Student-Newman-Keuls (SNK) *post hoc* test. Significance was determined if $p < 0.05$.

3. Results

3.1 mPFC and BLA inputs converge on the same DMS neurons

We studied mPFC and BLA inputs because although both inputs innervate the DMS and these three brain regions are closely involved in addiction (Balleine and O'Doherty, 2010; Corbit et al., 2013; Koob and Volkow, 2010), it is unclear how their glutamatergic transmission to the DMS is altered by excessive alcohol consumption. We first examined whether a DMS neuron received afferents from these two inputs. We infused an AAV expressing a channelrhodopsin, Chronos (Klapoetke et al., 2014), and GFP (AAV-Chronos-GFP) into the mPFC (Fig. 1A). In addition, we infused an A AV encoding another channelrhodopsin, Chrimson (Klapoetke et al., 2014), and the red fluorescent tdTomato protein (AAV-Chrimson-tdTomato) into the BLA of the same animals (Fig. 1B). DMS slices prepared 8 weeks after these infusions showed overlapping mPFC and BLA axonal fibers in a DMS region (Fig. 1C). Extensive axonal fibers and boutons projecting from each of these regions were observed in the same DMS area (Fig. 1C, right). The GFP (or tdTomato) signals were not results from fluorescence bleed-through from red (or green) channel (Supplementary Fig. 1).

Then, we examined whether these two different inputs targeted the same DMS neurons by using Chronos and Chrimson to selectively stimulate the mPFC and BLA afferents, respectively. To achieve this goal, we first examined whether the Chronos-mediated mPFC input was selectively activated by 405-nm light and the Chrimson-mediated BLA input by 590-nm light. Accumulating evidence suggests that the mPFC projects mainly to the anterior to middle region of the DMS and the BLA innervates the middle-posterior region (Corbit et al., 2013; Hunnicutt et al., 2016; Kelley et al., 1982; McDonald, 1991; Oh et al., 2014; Pan et al., 2010; Wall et al., 2013). We recorded neurons in an anterior DMS area that contained predominantly Chronos-GFP-containing fibers (Supplementary Fig. 2A–2C), and found that 405-nm light stimulation induced large excitatory postsynaptic currents (EPSCs) whereas 590-nm light did not (Fig. 1D, $t_{(6)} = 4.47$, $p < 0.01$). In contrast, when we recorded neurons in a posterior DMS area that mainly contained Chrimson-tdTomato-positive fibers (Supplementary Fig. 2D–2F), 590- but not 405-nm light evoked large EPSCs (Fig. 1E, $t_{(13)} = -5.17$, $p < 0.001$). These results suggest that in our experiments Chronos-expressing mPFC fibers and the Chrimson-containing inputs within the DMS can be selectively activated by 405- and 590-nm light, respectively.

Next, we recorded neurons in the middle portion of the DMS containing both the green and red fibers. As shown in Figure 1F, light stimulation of the mPFC and BLA induced responses in the same DMS neurons. In 22 neurons from 9 rats, 20 of them were responsive

to stimulation of both inputs, 2 neurons responded to the mPFC only, and no neurons responded to the BLA stimulation only (Fig. 1G). In addition, we found that optical stimulation of the Chronos-expressing mPFC input by 405-nm light evoked a large EPSC, whereas stimulation of the Chrimson-expressing BLA input using 590-nm light evoked a relatively small EPSC in the same DMS neurons (Fig. 1H). The amplitudes of the mPFC-derived EPSCs were significantly greater than those of the BLA-EPSCs in the same slices (Fig. 1I; $t_{(38)} = 3.38$, $p < 0.01$). Therefore, we focused most of our subsequent studies on the mPFC input. These results suggest that both the mPFC and BLA inputs could innervate the same population of medium spiny neurons in the DMS.

3.2 Excessive alcohol intake potentiates AMPAR-mediated mPFC inputs in rat DMS neurons

We recently reported that AMPAR-mediated spontaneous EPSCs in DMS neurons were potentiated by excessive alcohol intake (Wang et al., 2015). It is not known whether evoked EPSCs, particularly those elicited by activation of the mPFC input, are altered by alcohol. To address this question, we infused AAV-ChR2-tdTomato into the mPFC of adult rats and trained the animals to consume 20% alcohol for 8 weeks using the intermittent-access 2-bottle choice drinking procedure (Wang et al., 2012; Wang et al., 2010). Twenty-four hours after the last alcohol exposure, we prepared striatal slices and measured electrically-evoked AMPAR-EPSCs in the DMS. Specifically, we placed stimulating electrodes within the DMS area receiving fluorescent mPFC fibers, and measured AMPAR-EPSCs in DMS neurons using whole-cell recording. To compare the alcohol group and their water controls, we measured EPSCs in response to a range of electrical stimulation intensities (Fig. 2A, 2B). We found that the amplitude of electrically-evoked AMPAR-EPSCs was significantly higher in DMS neurons from the alcohol group than in those from the water group (Fig. 2B; $F_{(1,99)} = 8.80$, $p < 0.01$). This result suggests that excessive alcohol intake potentiates electrically-evoked AMPAR-EPSCs in DMS neurons.

We then delivered 405-nm light to selectively activate mPFC inputs and measured the specific corticostriatal AMPAR-EPSCs in DMS neurons from the alcohol and water groups (Fig. 2C, 2D). We found that the amplitude of mPFC-elicited AMPAR-EPSCs were significantly higher in the alcohol group than in the water group (Fig. 2D; $F_{(1, 104)} = 6.96$, $p < 0.05$). This result indicates that excessive alcohol consumption potentiates mPFC-derived AMPAR-mediated glutamatergic transmission in the DMS. Interestingly, we observed an all-or-none relationship between light-stimulation intensities and amygdalostriatal AMPAR-EPSC amplitudes (data not shown), which prevented us from exploring amygdalostriatal differences between water and alcohol groups.

3.3 Excessive alcohol intake potentiates NMDAR-mediated glutamatergic transmission elicited by the mPFC input to the rat DMS

The NMDAR is a well-characterized alcohol target that has been associated with alcohol drinking behavior (Lovinger et al., 1989; Wang et al., 2007). Chronic alcohol exposure has been shown to upregulate NMDAR function (Carpenter-Hyland and Chandler, 2006; Carpenter-Hyland et al., 2004; Kalluri et al., 1998; Kash et al., 2009; Wang et al., 2007; Wang et al., 2010). This increase in NMDAR function has been posited to play a role in the

hyperexcitable state (Hendricson et al., 2007) that is associated with alcohol withdrawal; however, no detailed analysis of the effects of chronic alcohol exposure on NMDAR activity at specific corticostriatal synapses has been performed. While measuring NMDAR-EPSCs, picrotoxin and NBQX were bath-applied to inhibit $GABA_A$ receptor-mediated and AMPAR-mediated responses. Electrical and optical stimulation-elicited NMDAR-EPSCs were measured at a variety of electrical intensities and stimulating laser powers. We found that the input-output relationship for electrically evoked NMDAR-EPSCs was much steeper in alcohol-treated rats than in those receiving water only (Fig. 3A, 3B; $F_{(1,104)} = 6.14$, $p < 0.05$ by two-way RM ANOVA). *Post hoc* analysis revealed significantly higher EPSC amplitudes at stimulating intensities of 160 (q = 3.79, $p < 0.01$) and 320 (q = 6.82, $p < 0.001$) μA in alcohol-treated rats, as compared to the water group. Measurement of optically evoked NMDAR-EPSCs from the mPFC input also identified a significantly higher input-output relationship in the alcohol group, as compared to the water controls (Fig. 3C, 3D; $F_{(1,76)} =$ 7,12, $p < 0.05$). *Post hoc* analysis demonstrated that the EPSC amplitude was higher at stimulating intensities of 0.5 (q = 4.57, $p < 0.01$) and 0.6 (q = 6.07, $p < 0.001$) mW in the alcohol-drinking rats, as compared with the water controls. These results suggest that excessive alcohol consumption potentiates synaptic NMDAR activity elicited by the mPFC input to the DMS.

3.4 Excessive alcohol intake selectively potentiates the GluN2B contribution to the mPFC input to the DMS

The NMDAR consists of GluN1 and GluN2 (A–D) subunits (Traynelis et al., 2010). *Ex vivo* and *in vivo* alcohol exposure has been shown to selectively upregulate the activity of GluN2B–containing NMDARs (Kash et al., 2009; Wang et al., 2007; Wang et al., 2011; Wang et al., 2010). Thus, we examined whether excessive alcohol intake altered the contribution of GluN2B to NMDAR-mediated synaptic responses in the DMS. We first measured electrically-evoked NMDAR-EPSCs in the absence and presence of a GluN2B antagonist, Ro 25–6981, and calculated the GluN2B/NMDAR ratio (see Methods for the detailed calculation). We found the ratio was significantly increased in the alcohol group, as compared to the water group (Fig. 4; 0.59 ± 0.04 for Alcohol versus 0.47 ± 0.03 for Water. $t_{(26)} = -2.44$, $p < 0.05$). Since electrically-evoked EPSCs contain both mPFC and BLA inputs, we then optogenetically stimulated each afferent and measured corticostriatal and amygdalostriatal GluN2B/NMDAR ratios. Interestingly, we discovered that the ratio was significantly increased at the mPFC, but not BLA input in alcohol-drinking rats, as compared to their water controls (Fig. 4; Corticostriatal: 0.58 ± 0.03 for Water versus 0.75 ± 0.03 for Alcohol, $t_{(24)} = -4.31$, $p < 0.001$; Amygdalostriatal: 0.59 ± 0.07 for Water versus 0.61 ± 0.07 for Alcohol, $t_{(13)} = -0.17$, $p > 0.05$). These results indicate that excessive alcohol intake potentiates GluN2B activity selectively at the site of mPFC input within the DMS.

3.5 Excessive alcohol intake enhances glutamate release probability selectively at the BLA input to the DMS

In addition to measuring postsynaptic alterations, we also assessed whether excessive alcohol intake changed the probability of presynaptic glutamate release. We measured the PPRs of EPSCs that were activated by two stimuli, delivered 100 ms apart. We found that

the PPR for electrically-evoked EPSCs, or for optically-evoked corticostriatal EPSCs, did not differ between the alcohol group and their water controls (Fig. 5; electrical: $t_{(42)} = 1.38$, $p > 0.05$; corticostriatal: $t_{(30)} = 0.87$, $p > 0.05$). However, the PPR for the BLA input was significantly lower in the alcohol-drinking rats than in the water controls (Fig. 5; $t_{(15)} = 2.57$, $p < 0.05$). Since the PPR is inversely correlated with transmitter release probability (Zucker and Regehr, 2002), this reduced PPR indicates an increase in glutamate release. Together, these results suggest that excessive alcohol intake enhances the probability of glutamate release selectively at the BLA afferents within the DMS.

3.6 Pairing of mPFC and BLA afferents induces corticostriatal LTP in the DMS

Drug evoked-plasticity has been reported to share the same mechanism with LT P (Luscher and Malenka, 2011). To further explore the potential mechanism of alcohol-evoked plasticity, we investigated LT P induction at corticostriatal synapses, which are thought to contribute to the development of alcohol use disorder (Barker et al., 2015; Lovinger and Kash, 2015). However, corticostriatal LTP cannot be reliably induced in the striatum of adult rats (Lovinger, 2010). Interestingly, electrical stimulation studies reported that the BLA input regulated corticostriatal neurotransmission at posterior striatal neurons (Popescu et al., 2007). The present study employed optogenetic stimulation to examine whether the BLA input regulated mPFC afferents in the DMS. Eight weeks after the infusion of AAV-Chronos-GFP into the mPFC and AAV-Chrimson-tdTomato into the BLA, DMS slices were prepared. We selected medium spiny neurons in the GFP- and tdTomato-expressing DMS area, and stimulated each input using different wavelengths of light. The recordings were conducted with an intracellular solution containing the sodium channel blocker QX-314 to block generation of action potentials. As shown in Figure 6A, optical stimulation of either the mPFC or BLA input induced an EPSP. Simultaneous stimulation of both inputs induced a large membrane depolarization that was abolished by a cocktail of an AMPAR antagonist, NBQX, and a NMDAR antagonist, APV (Fig. 6A right), suggesting that the depolarization was induced by glutamatergic transmission. In addition, we found that the duration of larger depolarization by co-activation of both inputs was partially reduced by a voltage-gated calcium channel blocker, $NiCl_2$ (Supplementary Fig. S3; $t_{(3)} = 6.76$, $p < 0.01$). When comparing membrane depolarization in response to individual inputs and co-activation, we found that the amplitude of large membrane depolarization was significantly greater than the sum of the peak amplitudes of the individual responses following stimulation of either mPFC or BLA inputs (Fig. 6B, 6C left; $t_{(5)} = -3.70$, $p < 0.05$). Similarly, the area under the large depolarization curve was significantly greater than the sum of the area under the individual responses (Fig. 6C middle; $t_{(5)} = -2.88$, $p < 0.05$). In contrast, the decay time between the large depolarization and the summed response did not differ (Fig. 6C right; $t_{(5)} = -1.04$, $p > 0.05$). Together, these results suggest that co-activation of the mPFC and BLA inputs induced a synergistic effect on the membrane depolarization in DMS neurons.

Next, we tested whether pairing of the mPFC and BLA inputs induced LTP. After stable baseline recordings of corticostriatal fEPSP/PS were achieved, mPFC and BLA stimulation was paired for 2 sec at 50 Hz, and corticostriatal fEPSP/PS were then continuously recorded for 40 min. As shown in Figure 6D, pairing of the mPFC and the BLA input induced reliable LTP (average fEPSP/PS amplitude 30–40 min post-induction: 113.78 ± 4.41% of baseline,

$t_{(7)} = -3.13$, $p < 0.05$). In contrast, light stimulation of the BLA input alone did not induce corticostriatal LTP (average fEPSP/PS amplitude post-induction: 95.24 ± 5.21% of baseline, $t_{(5)} = 0.91$, $p > 0.05$). The average fEPSP/PS amplitude 30–40 min post-induction was significantly higher after co-stimulation of the mPFC and BLA input than after BLA stimulation alone ($t_{(12)} = 2.73$, $p < 0.05$). This result suggests that co-activation of the BLA and mPFC afferents reliably induces corticostriatal LTP. Lastly, we found that the LT P was completely blocked by the GluN2B antagonist, Ro 25–6981 (Fig. 6E; 96.91 ± 2.85% of baseline, $t_{(4)} = 1.09$, $p > 0.05$), suggesting that the corticostriatal LTP is GluN2B–dependent.

4. Discussion

The present study demonstrated that both the mPFC and BLA inputs targeted the same DMS neurons. In addition, we found that excessive alcohol intake potentiated AMPAR- and NMDAR-mediated synaptic transmission at the mPFC input, and increased the probability of glutamate release at the BLA afferents (Fig. 7). These results indicate that excessive alcohol consumption specifically alters postsynaptic aspects of corticostriatal glutamatergic neurotransmission and presynaptic aspects of amygdalostriatal neurotransmission. These changes may, in turn, contribute to pathological alcohol consumption. Importantly, co-activation of the mPFC and BLA inputs reliably induced corticostriatal LTP, a plasticity involved in goal-directed behavior and drug addiction (Balleine and O'Doherty, 2010; Lovinger, 2010).

4.1 Converging inputs from the mPFC and BLA onto the DMS

Although it has long been known that both the mPFC and BLA project to the DMS (Corbit et al., 2013; Hunnicutt et al., 2016; Kelley et al., 1982; McDonald, 1991; Oh et al., 2014; Pan et al., 2010; Wall et al., 2013), we demonstrated for the first time that both inputs overlapped in some DMS areas and targeted the same neuronal population. Previous studies used a single tracer to examine either the mPFC or BLA input; in this study, we employed two viruses encoding different fluorescence proteins (i.e., GFP and tdTomato) to label mPFC and BLA afferents in the same section. One concern about such double labeling is that the fluorescence of one protein (e.g., GFP) may bleed through into the other channel (e.g., tdTomato). However, we observed very weak fluorescence signals in the second channel when we expressed one protein at a time. The weak fluorescent signals were also observed in a far-red channel, indicating they were auto-fluorescence and not bleed-through fluorescent signals. Using electrical stimulation of posterior coronal sections containing the cortex, BLA, and striatum, Popescu et al. (2007) demonstrated that inputs from both the cortex and the BLA targeted the same striatal neurons. However, the limitations of electrical stimulation only allowed them to confirm the convergent inputs from the posterior cortex and BLA to the striatum. Since then, optogenetics has been used to investigate the mPFC and BLA inputs to the ventral striatum at desired anterior-posterior sections (Britt et al., 2012; Joffe and Grueter, 2016; Lee et al., 2013; Ma et al., 2014; MacAskill et al., 2014; Pascoli et al., 2014). However, the limitations of single-channel optogenetics only allowed them to study one input in the same recording. Dual-channel optogenetics enables measurement of two synaptic transmissions in the same recording (Klapoetke et al., 2014;

Yizhar et al., 2011). Using this technique, we found that the mPFC and BLA inputs innervated the same DMS neurons, with a greater strength from the mPFC input.

4.2 Alcohol potentiates glutamatergic inputs from the mPFC and BLA via different mechanisms

We previously reported that excessive alcohol intake increased the amplitude of miniature EPSCs in DMS neurons (Wang et al., 2015) and it was therefore unsurprising that the present study identified an increase in electrically-evoked AMPAR-mediated EPSCs. However, optogenetically evoked AMPAR-EPSCs from the mPFC input were also potentiated, suggesting that the increase in electrically-evoked AMPAR-EPSCs arose, at least in part, from the mPFC input. Similarly, an increase in electrically-evoked NMDAR-EPSCs was reported previously (Wang et al., 2010) and the present study found an alcohol-mediated increase that also resulted, at least partially, from the mPFC input, because optogenetically evoked NMDAR-EPSCs from this input were potentiated. Furthermore, the increased NMDAR activity was associated with an increased contribution of GluN2B–containing receptors to electrically-evoked EPSCs; this was consistent with a previous finding that excessive alcohol consumption increased GluN2B phosphorylation and activity (Wang et al., 2010). Again, the increased corticostriatal GluN2B/NMDAR ratio indicated that this change occurred, at least in part, at the site of the mPFC input.

Interestingly, while we found increases in corticostriatal AMPAR- and NMDAR-EPSCs, we did not detect a change in PPR. This indicates that this alcohol-induced glutamatergic change occurred predominantly at a postsynaptic site, i.e., via a modification of AMPAR and/or NMDAR responsiveness. This is consistent with our recent finding that AMPA- or NMDA-induced currents, as well as the mEPSC amplitude, were increased following excessive alcohol intake (Cheng et al., 2016; Wang et al., 2015). As for the BLA input, we found an alcohol-mediated decrease in the PPR, indicating an increased probability of glutamate release. This is congruent with previous reports of an increased mEPSC frequency following excessive alcohol consumption or cocaine administration (MacAskill et al., 2014; Wang et al., 2015). We observed a smaller PPR of optogenetically-evoked EPSCs (< 1.0) than that of electrically-evoked EPSCs (> 1.0), which is in line with previous studies (Ding et al., 2008; Wu et al., 2015). The small PPR of optogenetic EPSCs may result from strong inactivation and desensitization of ChR2 used (Lin et al., 2009); for instance, ChR2-mediated response cannot follow light stimulation above 20 Hz (Wu et al., 2015). In fact, when Chronos, a channelrhodopsin with a faster kinetic than ChR2, was employed, the PPR was greater than 1.0 (Klapoetke et al., 2014). In addition, dopamine D2 receptor activation, which likely occurs in electrical but not optical stimulation, causes a decrease in the probability of striatal glutamate release and thus an increase in PPR (Yin and Lovinger, 2006). The lack of D2 receptor activation may also contribute to a small PPR of optogenetically-evoked corticostriatal EPSCs. Nevertheless, alcohol consumption potentiated the mPFC inputs through a postsynaptic mechanism and enhanced BLA inputs via a presynaptic mechanism.

4.3 Alcohol-induced plasticity, LTP, and mPFC and BLA afferents in the DMS

We observed that excessive alcohol consumption potentiated corticostriatal AMPAR-mediated synaptic transmission. This alcohol-evoked synaptic plasticity may occur through two different but related mechanisms. First, alcohol consumption may potentiate corticostriatal AMPAR response through a GluN2B–dependent mechanism, given that alcohol enhancement of GluN2B was reported to facilitate LTP induction in the DMS (Wang et al., 2012; Wills et al., 2012). Second, the synergistic effect of simultaneous corticostriatal and amygdalostriatal inputs on membrane depolarization helps reliably induce LTP. Co-activation of both inputs caused a larger membrane depolarization than the sum of depolarization elicited by individual inputs. The large membrane depolarization is expected to strongly remove Mg^{2+} blockade of NMDAR channels, leading to large calcium influx, and consequently reliable LTP induction. Alcohol enhancement of amygdalostriatal glutamate release may contribute to alcohol-evoked plasticity through this LTP mechanism. Furthermore, the LTP is GluN2B–dependent, which is consistent with alcohol-mediated GluN2B enhancement in this and previous studies (Kash et al., 2009; Wang et al., 2011; Wang et al., 2010; Wills et al., 2012).

4.4 Implication for alcohol use disorder

Since corticostriatal plasticity is essential for strengthening action-outcome association in goal-directed learning (Balleine and O'Doherty, 2010), alcohol-mediated synaptic plasticity at the corticostriatal input may contribute to goal-directed actions in alcohol-drinking behavior. Importantly, the amygdalostriatal input in the DMS is also required for the acquisition and expression of goal-directed actions (Corbit et al., 2013). In this study, we discovered that alcohol intake potentiated amygdalostriatal glutamate release and that amygdalostriatal and corticostriatal co-activation reliably induced LTP, suggesting that the BLA input may contribute to goal-directed actions by promoting corticostriatal plasticity. In addition, it is well known that the BLA contributes to relapse to drug and alcohol abuse (Koob, 2008), and a recent study found that the DMS was also involved in relapse (Caprioli et al., 2017). The BLA input may enhance corticostriatal transmission, leading to relapse to alcohol. Drug-induced synaptic plasticity is thought to share the same mechanism with LTP, which represents a long-lasting increase in the efficacy of glutamatergic synapses (Lovinger, 2010; Luscher and Malenka, 2011). Therefore, we can infer that alcohol-induced corticostriatal and amygdalostriatal plasticity will promote goal-directed actions in excessive alcohol intake and relapse.

5. Conclusions

In summary, the present study showed that the mPFC and BLA inputs innervate the same DMS neurons and that co-activation of the mPFC and BLA inputs reliably resulted in corticostriatal LTP. Furthermore, excessive alcohol intake potentiates postsynaptic glutamatergic activity at the site of the mPFC input and increases the probability of glutamate release at the BLA afferent. These changes may contribute to pathological alcohol consumption.

Supplementary Material

Refer to Web version on PubMed Central for supplementary material.

Acknowledgments

This research was supported by grants from NIAAA AA021505 and R01AA024659.

Abbreviations

AAV	adeno-associated virus
ChR2	channelrhodopsin 2
GFP	green fluorescent protein
DMS	dorsomedial striatum
mPFC	medial prefrontal cortex
BLA	basolateral amygdala
EPSC	excitatory postsynaptic current
EPSP	excitatory postsynaptic potential
fEPSP/PS	field excitatory postsynaptic potentials/population spikes
NMDAR	NMDA receptor
AMPAR	AMPA receptor
LTP	long-term potentiation

References

Balleine BW, O'Doherty JP. Human and rodent homologies in action control: corticostriatal determinants of goal-directed and habitual action. Neuropsychopharmacology. 2010; 35:48–69. [PubMed: 19776734]

Barker JM, Corbit LH, Robinson DL, Gremel CM, Gonzales RA, Chandler LJ. Corticostriatal circuitry and habitual ethanol seeking. Alcohol. 2015; 49:817–824. [PubMed: 26059221]

Britt JP, Benaliouad F, McDevitt RA, Stuber GD, Wise RA, Bonci A. Synaptic and behavioral profile of multiple glutamatergic inputs to the nucleus accumbens. Neuron. 2012; 76:790–803. [PubMed: 23177963]

Caprioli D, Venniro M, Zhang M, Bossert JM, Warren BL, Hope BT, Shaham Y. Role of Dorsomedial Striatum Neuronal Ensembles in Incubation of Methamphetamine Craving after Voluntary Abstinence. J Neurosci. 2017; 37:1014–1027. [PubMed: 28123032]

Carpenter-Hyland EP, Chandler LJ. Homeostatic plasticity during alcohol exposure promotes enlargement of dendritic spines. Eur J Neurosci. 2006; 24:3496–3506. [PubMed: 17229098]

Carpenter-Hyland EP, Woodward JJ, Chandler LJ. Chronic ethanol induces synaptic but not extrasynaptic targeting of NMDA receptors. J Neurosci. 2004; 24:7859–7868. [PubMed: 15356198]

Cheng Y, Huang CC, Ma T, Wei X, Wang X, Lu J, Wang J. Distinct Synaptic Strengthening of the Striatal Direct and Indirect Pathways Drives Alcohol Consumption. Biol Psychiatry. 2016 [Epub ahead of print].

Corbit LH, Chieng BC, Balleine BW. Effects of repeated cocaine exposure on habit learning and reversal by N-acetylcysteine. Neuropsychopharmacology. 2014; 39:1893–1901. [PubMed: 24531561]

Corbit LH, Leung BK, Balleine BW. The role of the amygdala-striatal pathway in the acquisition and performance of goal-directed instrumental actions. J Neurosci. 2013; 33:17682–17690. [PubMed: 24198361]

Ding J, Peterson JD, Surmeier DJ. Corticostriatal and thalamostriatal synapses have distinctive properties. J Neurosci. 2008; 28:6483–6492. [PubMed: 18562619]

Gerdeman GL, Partridge JG, Lupica CR, Lovinger DM. It could be habit forming: drugs of abuse and striatal synaptic plasticity. Trends Neurosci. 2003; 26:184–192. [PubMed: 12689769]

Hendricson AW, Maldve RE, Salinas AG, Theile JW, Zhang TA, Diaz LM, Morrisett RA. Aberrant synaptic activation of N-methyl-D-aspartate receptors underlies ethanol withdrawal hyperexcitability. J Pharmacol Exp Ther. 2007; 321:60–72. [PubMed: 17229881]

Hunnicutt BJ, Jongbloets BC, Birdsong WT, Gertz KJ, Zhong H, Mao T. A comprehensive excitatory input map of the striatum reveals novel functional organization. Elife. 2016:5.

Joffe ME, Grueter BA. Cocaine Experience Enhances Thalamo-Accumbens N-Methyl-D-Aspartate Receptor Function. Biol Psychiatry. 2016; 80:671–681. [PubMed: 27209241]

Kalluri HS, Mehta AK, Ticku MK. Up-regulation of NMDA receptor subunits in rat brain following chronic ethanol treatment. Brain Res Mol Brain Res. 1998; 58:221–224. [PubMed: 9685652]

Kash TL, Baucum AJ 2nd, Conrad KL, Colbran RJ, Winder DG. Alcohol exposure alters NMDAR function in the bed nucleus of the stria terminalis. Neuropsychopharmacology. 2009; 34:2420–2429. [PubMed: 19553918]

Kelley AE, Domesick VB, Nauta WJ. The amygdalostriatal projection in the rat--an anatomical study by anterograde and retrograde tracing methods. Neuroscience. 1982; 7:615–630. [PubMed: 7070669]

Klapoetke NC, Murata Y, Kim SS, Pulver SR, Birdsey-Benson A, Cho YK, Morimoto TK, Chuong AS, Carpenter EJ, Tian Z, Wang J, Xie Y, Yan Z, Zhang Y, Chow BY, Surek B, Melkonian M, Jayaraman V, Constantine-Paton M, Wong GK, Boyden ES. Independent optical excitation of distinct neural populations. Nat Methods. 2014; 11:338–346. [PubMed: 24509633]

Koob GF. A role for brain stress systems in addiction. Neuron. 2008; 59:11–34. [PubMed: 18614026]

Koob GF, Volkow ND. Neurocircuitry of addiction. Neuropsychopharmacology. 2010; 35:217–238. [PubMed: 19710631]

Kupferschmidt DA, Cody PA, Lovinger DM, Davis MI. Brain BLAQ: Post-hoc thick-section histochemistry for localizing optogenetic constructs in neurons and their distal terminals. Front Neuroanat. 2015; 9:6. [PubMed: 25698938]

Lee BR, Ma YY, Huang YH, Wang X, Otaka M, Ishikawa M, Neumann PA, Graziane NM, Brown TE, Suska A, Guo C, Lobo MK, Sesack SR, Wolf ME, Nestler EJ, Shaham Y, Schluter OM, Dong Y. Maturation of silent synapses in amygdala-accumbens projection contributes to incubation of cocaine craving. Nat Neurosci. 2013; 16:1644–1651. [PubMed: 24077564]

Lin JY, Lin MZ, Steinbach P, Tsien RY. Characterization of engineered channelrhodopsin variants with improved properties and kinetics. Biophys J. 2009; 96:1803–1814. [PubMed: 19254539]

Lovinger DM. Neurotransmitter roles in synaptic modulation, plasticity and learning in the dorsal striatum. Neuropharmacology. 2010; 58:951–961. [PubMed: 20096294]

Lovinger DM, White G, Weight FF. Ethanol inhibits NMDA-activated ion current in hippocampal neurons. Science. 1989; 243:1721–1724. [PubMed: 2467382]

Lovinger DMPD, Kash TLPD. Mechanisms of Neuroplasticity and Ethanol's Effects on Plasticity in the Striatum and Bed Nucleus of the Stria Terminalis. Alcohol Res. 2015; 37:109–124. [PubMed: 26259092]

Luscher C, Malenka RC. Drug-evoked synaptic plasticity in addiction: from molecular changes to circuit remodeling. Neuron. 2011; 69:650–663. [PubMed: 21338877]

Ma YY, Lee BR, Wang X, Guo C, Liu L, Cui R, Lan Y, Balcita-Pedicino JJ, Wolf ME, Sesack SR, Shaham Y, Schluter OM, Huang YH, Dong Y. Bidirectional Modulation of Incubation of Cocaine Craving by Silent Synapse-Based Remodeling of Prefrontal Cortex to Accumbens Projections. Neuron. 2014; 83:1453–1467. [PubMed: 25199705]

MacAskill AF, Cassel JM, Carter AG. Cocaine exposure reorganizes cell type- and input-specific connectivity in the nucleus accumbens. Nat Neurosci. 2014; 17:1198–1207. [PubMed: 25108911]

McDonald AJ. Organization of amygdaloid projections to the prefrontal cortex and associated striatum in the rat. Neuroscience. 1991; 44:1–14. [PubMed: 1722886]

Oh SW, Harris JA, Ng L, Winslow B, Cain N, Mihalas S, Wang Q, Lau C, Kuan L, Henry AM, Mortrud MT, Ouellette B, Nguyen TN, Sorensen SA, Slaughterbeck CR, Wakeman W, Li Y, Feng D, Ho A, Nicholas E, Hirokawa KE, Bohn P, Joines KM, Peng H, Hawrylycz MJ, Phillips JW, Hohmann JG, Wohnoutka P, Gerfen CR, Koch C, Bernard A, Dang C, Jones AR, Zeng H. A mesoscale connectome of the mouse brain. Nature. 2014; 508:207–214. [PubMed: 24695228]

Pan WX, Mao T, Dudman JT. Inputs to the dorsal striatum of the mouse reflect the parallel circuit architecture of the forebrain. Front. Neuroanat. 2010; 4:147.

Pascoli V, Terrier J, Espallergues J, Valjent E, O'Connor EC, Luscher C. Contrasting forms of cocaine-evoked plasticity control components of relapse. Nature. 2014; 509:459–464. [PubMed: 24848058]

Paxinos, G., Watson, C. The Rat Brain in stereotaxic coordinates. Academic Press; San Diego: 2007.

Popescu AT, Saghyan AA, Pare D. NMDA-dependent facilitation of corticostriatal plasticity by the amygdala. Proc Natl Acad Sci U S A. 2007; 104:341–346. [PubMed: 17182737]

Seif T, Chang SJ, Simms JA, Gibb SL, Dadgar J, Chen BT, Harvey BK, Ron D, Messing RO, Bonci A, Hopf FW. Cortical activation of accumbens hyperpolarization-active NMDARs mediates aversion-resistant alcohol intake. Nat Neurosci. 2013; 16:1094–1100. [PubMed: 23817545]

Traynelis SF, Wollmuth LP, McBain CJ, Menniti FS, Vance KM, Ogden KK, Hansen KB, Yuan H, Myers SJ, Dingledine R. Glutamate receptor ion channels: structure, regulation, and function. Pharmacol Rev. 2010; 62:405–496. [PubMed: 20716669]

Wall NR, De La Parra M, Callaway EM, Kreitzer AC. Differential innervation of direct-and indirect-pathway striatal projection neurons. Neuron. 2013; 79:347–360. [PubMed: 23810541]

Wang J, Ben Hamida S, Darcq E, Zhu W, Gibb SL, Lanfranco MF, Carnicella S, Ron D. Ethanol-mediated facilitation of AMPA receptor function in the dorsomedial striatum: implications for alcohol drinking behavior. J Neurosci. 2012; 32:15124–15132. [PubMed: 23100433]

Wang J, Carnicella S, Phamluong K, Jeanblanc J, Ronesi JA, Chaudhri N, Janak PH, Lovinger DM, Ron D. Ethanol induces long-term facilitation of NR2B–NMDA receptor activity in the dorsal striatum: implications for alcohol drinking behavior. J Neurosci. 2007; 27:3593–3602. [PubMed: 17392475]

Wang J, Cheng Y, Wang X, Roltsch Hellard E, Ma T, Gil H, Ben Hamida S, Ron D. Alcohol Elicits Functional and Structural Plasticity Selectively in Dopamine D1 Receptor-Expressing Neurons of the Dorsomedial Striatum. J Neurosci. 2015; 35:11634–11643. [PubMed: 26290240]

Wang J, Lanfranco MF, Gibb SL, Ron D. Ethanol-mediated long-lasting adaptations of the NR2B–containing NMDA receptors in the dorsomedial striatum. Channels (Austin). 2011; 5:205–209. [PubMed: 21289476]

Wang J, Lanfranco MF, Gibb SL, Yowell QV, Carnicella S, Ron D. Long-lasting adaptations of the NR2B–containing NMDA receptors in the dorsomedial striatum play a crucial role in alcohol consumption and relapse. J Neurosci. 2010; 30:10187–10198. [PubMed: 20668202]

Wang J, Yeckel MF, Johnston D, Zucker RS. Photolysis of postsynaptic caged Ca^{2+} can potentiate and depress mossy fiber synaptic responses in rat hippocampal CA3 pyramidal neurons. J Neurophysiol. 2004; 91:1596–1607. [PubMed: 14645386]

Wills TA, Klug JR, Silberman Y, Baucum AJ, Weitlauf C, Colbran RJ, Delpire E, Winder DG. GluN2B subunit deletion reveals key role in acute and chronic ethanol sensitivity of glutamate synapses in bed nucleus of the stria terminalis. Proc Natl Acad Sci U S A. 2012; 109:E278–287. [PubMed: 22219357]

Wu YW, Kim JI, Tawfik VL, Lalchandani RR, Scherrer G, Ding JB. Input- and cell-type-specific endocannabinoid-dependent LTD in the striatum. Cell Rep. 2015; 10:75–87. [PubMed: 25543142]

Yin HH, Knowlton BJ. The role of the basal ganglia in habit formation. Nat Rev Neurosci. 2006; 7:464–476. [PubMed: 16715055]

Yin HH, Lovinger DM. Frequency-specific and D2 receptor-mediated inhibition of glutamate release by retrograde endocannabinoid signaling. Proc Natl Acad Sci U S A. 2006; 103:8251–8256. [PubMed: 16698932]

Yizhar O, Fenno LE, Prigge M, Schneider F, Davidson TJ, O'Shea DJ, Sohal VS, Goshen I, Finkelstein J, Paz JT, Stehfest K, Fudim R, Ramakrishnan C, Huguenard JR, Hegemann P, Deisseroth K. Neocortical excitation/inhibition balance in information processing and social dysfunction. Nature. 2011; 477:171–178. [PubMed: 21796121]

Zucker RS, Regehr WG. Short-term synaptic plasticity. Annu Rev Physiol. 2002; 64:355–405. [PubMed: 11826273]

Highlights

- mPFC and BLA afferents innervate the same DMS neurons.
- Excessive alcohol intake enhances glutamate receptor activity at mPFC→DMS synapses.
- Excessive alcohol intake potentiates glutamate release at BLA→DMS synapses.
- Co-activation of mPFC and BLA inputs results in LTP at mPFC→DMS synapses.

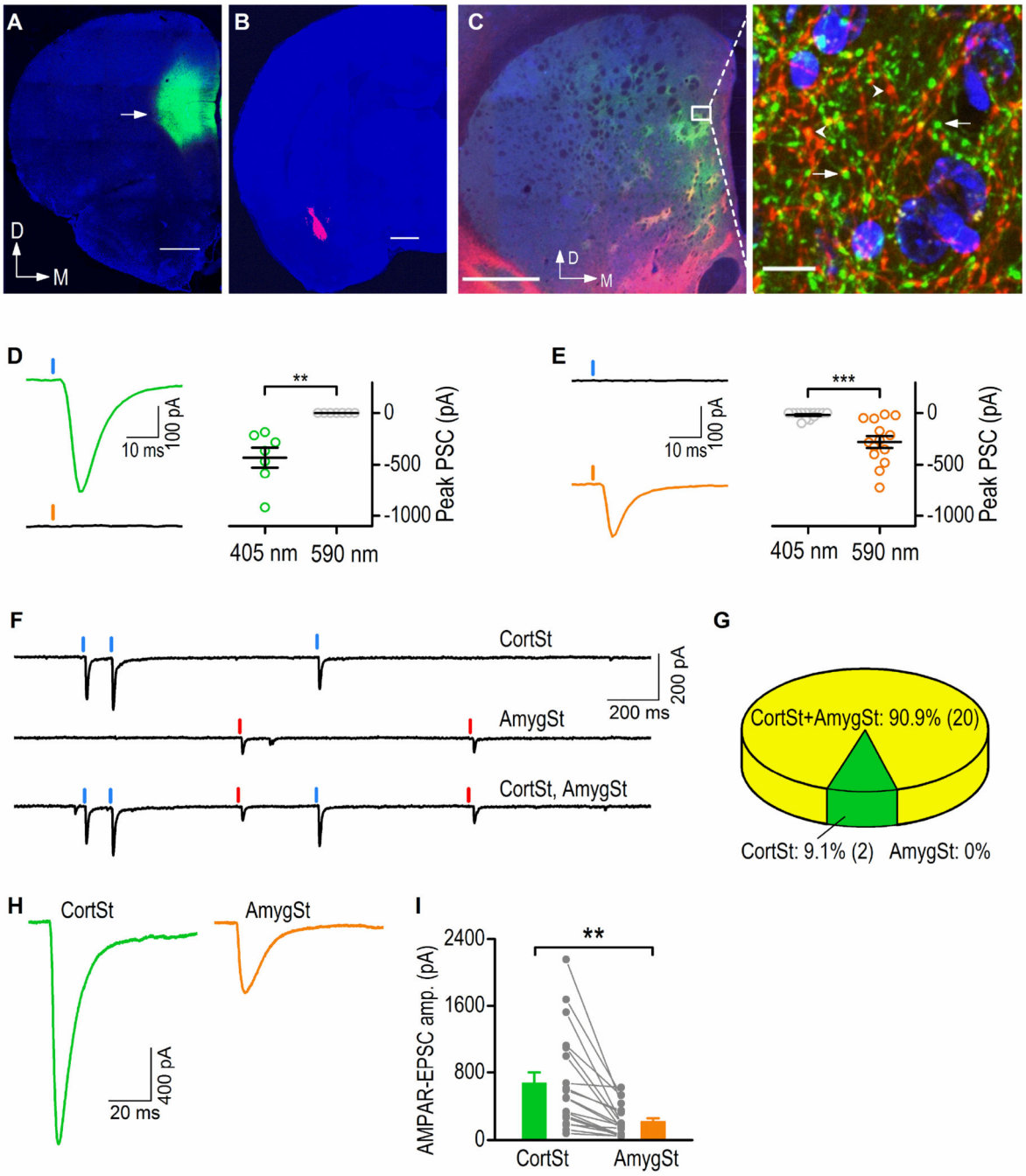

Fig. 1. Comparison of corticostriatal and amygdalostriatal synaptic inputs to the DMS

Coronal sections were prepared 8 weeks after the infusion of viral vectors into the rat mPFC (AAV-Chronos-GFP) and BLA (AAV-Chrimson-tdTomato). (A–B) Fluorescent micrographs showing the infusion sites of the mPFC (A) and BLA (B). The sections were counterstained with DAPI (Blue). The arrow indicates the fluorescence of GFP (A) and tdTomato (B) proteins expressed in the mPFC and BLA, respectively. D, dorsal; M, medial. Scale bar: 1 mm. (C) Fluorescent micrograph (left-hand panel) showing the co-innervation of the DMS by afferents from the mPFC (green) and BLA (red). Scale bar: 1 mm. The boxed area is

presented at higher magnification in the right-hand panel, showing the overlap of the green mPFC and red BLA axonal terminals. Note the extensive terminal boutons from the mPFC axons (arrows) and the BLA axons (arrowheads). Scale bar: 10 mm. (D) Chronos-driven excitatory postsynaptic currents (EPSCs) under 405- or 590-nm light, obtained from a representative neuron (left), with population data (right). $^{**}p < 0.01$, paired *t* test. n = 7 neurons from 3 rats. (E) Chrimson-driven EPSCs under 405- or 590-nm light, obtained from a representative neuron (left), with population data (right). $^{***}p < 0.01$, paired *t* test, n = 14 neurons from 3 rats. (F) AMPAR-EPSCs in response to optical stimulation of corticostriatal (CortSt) and amygdalostriatal (AmygSt) inputs within the DMS. Sample trace showing the AMPAR-EPSCs from a single neuron experiencing CortSt (top), AmygSt (center), and both input (bottom) stimulation. (G) Summary of percentages of neurons that received CortSt inputs, AmygSt inputs, and both. n = 22 neurons from 9 rats. (H) Representative traces of optogenetically-evoked EPSCs observed following light-induced stimulation of the CortSt and AmygSt inputs. (I) Bar graph comparing the individual and averaged EPSC amplitudes generated by CortSt and AmygSt activation. $^{**}p < 0.01$, unpaired *t* test. n = 20 neurons from 9 rats per group.

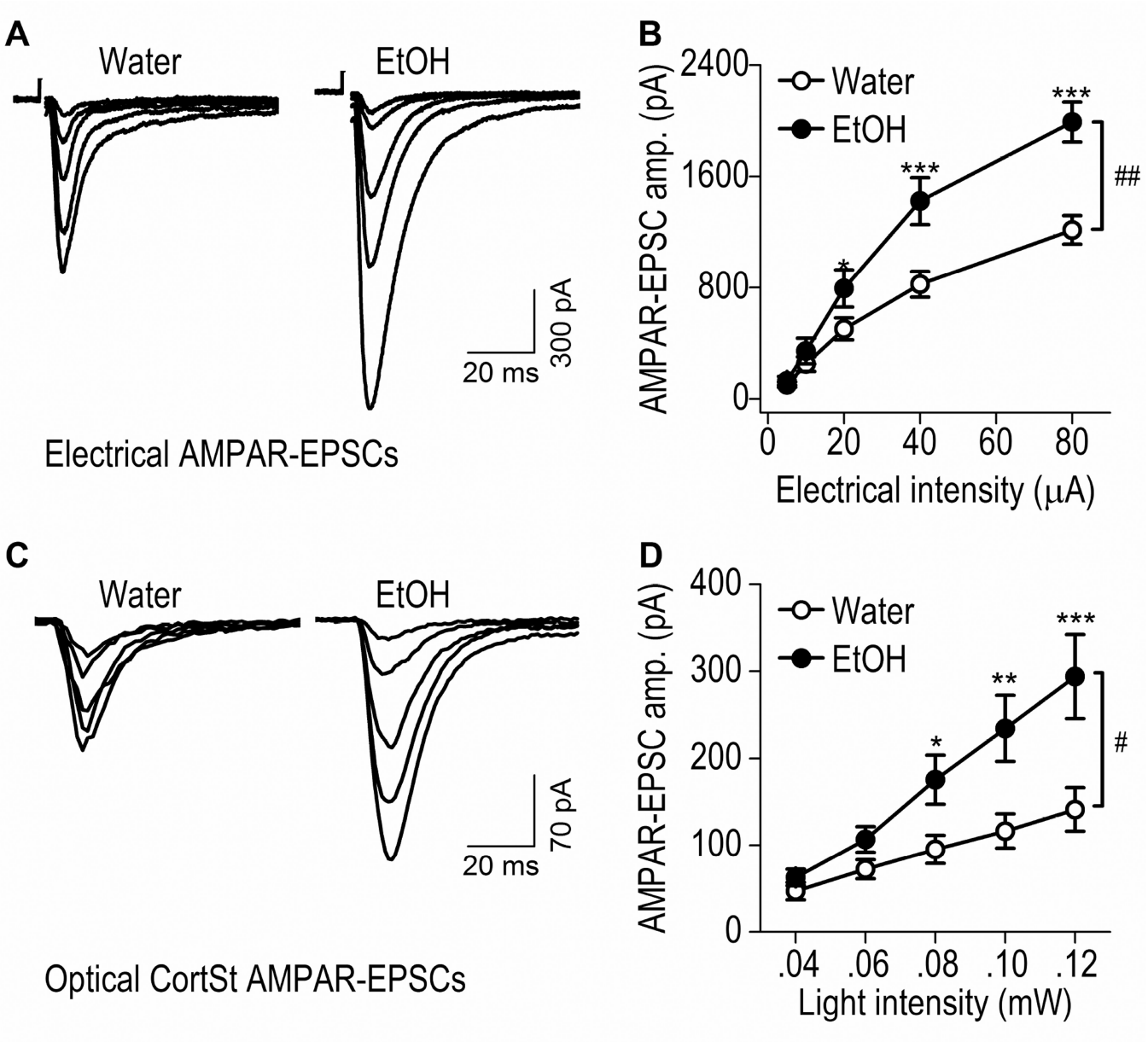

Fig. 2. Excessive alcohol intake increases corticostriatal AMPAR-mediated EPSCs within the rat DMS

AAV-ChR2-tdTomato was infused into the mPFC of rats that were then trained to consume 20% alcohol for 8 weeks using the intermittent-access 2-bottle-choice drinking procedure; DMS slices were prepared 1 d after the last drinking session. Whole-cell recording was used to detect AMPAR-EPSCs in DMS neurons following electrical (A, B) or optical (C, D; 470 nm) stimulation. (A) Representative traces of AMPAR-EPSCs evoked by indicated electrical stimulation intensities in slices from alcohol-drinking rats (EtOH) and water controls. (B) Input-output curves of electrical AMPAR-EPSCs in DMS neurons from rats exposed to alcohol or water only. $^{\#\#}p < 0.01$; two-way RM-ANOVA. $^{*}p < 0.05$ and $^{***}p < 0.001$ vs. Water at the same stimulation intensity; *post hoc* SNK tests. n = 14 neurons from 7 rats for Water and 13 neurons from 7 rats for EtOH. (C) Sample traces of CortSt AMPAR-EPSCs

evoked by the indicated optical stimulation intensities in slices from alcohol-drinking rats and water controls. (D) Input-output curves of CortSt AMPAR-EPSCs in DMS neurons from rats exposed to alcohol or water only. $^{\#}p < 0.05$, two-way RM-ANOVA. $^{*}p < 0.05$, $^{**}p < 0.01$, and $^{***}p < 0.001$ vs. Water at the same stimulating intensity; *post hoc* SNK tests. n = 14 neurons from 9 rats for Water and 14 neurons from 8 rats for EtOH.

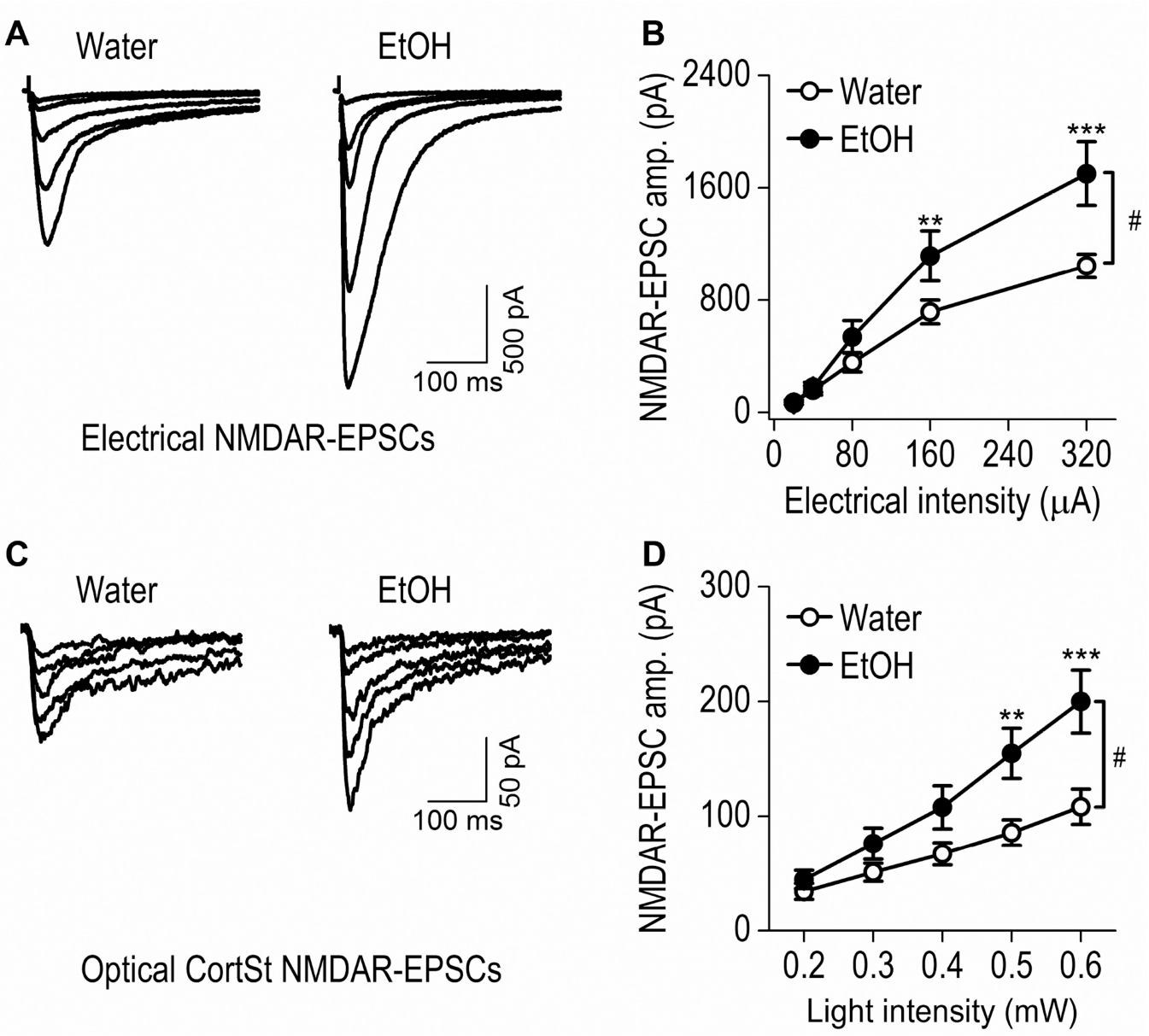

Fig. 3. Excessive alcohol intake increases corticostriatal NMDAR-mediated EPSCs within the rat DMS

(A) Representative traces of NMDAR-EPSCs evoked by the indicated electrical stimulation intensities in slices from alcohol-drinking rats and water controls. (B) Input-output curves of electrical NMDAR-EPSCs in DMS neurons from the indicated study groups. $^{\#}p < 0.05$; Two-way RM-ANOVA. $^{**}p < 0.01$ and $^{***}p < 0.001$ vs. Water at the same stimulation intensity, *post hoc* SNK tests. n = 15 neurons from 7 rats for Water and 13 neurons from 7 rats for EtOH. (C) Sample traces of CortSt NMDAR-EPSCs evoked by the indicated optical stimulation intensities in slices from water controls and alcohol-drinking rats. (D) Input-output curves of CortSt NMDAR-EPSCs in DMS neurons from the indicated study groups. $^{\#}p < 0.05$; Two-way RM-ANOVA. $^{**}p < 0.01$ and $^{***}p < 0.001$ versus Water at the

same stimulation intensity; *post hoc* SNK tests. n = 11 neurons from 7 rats for Water and 10 neurons from 6 rats for EtOH.

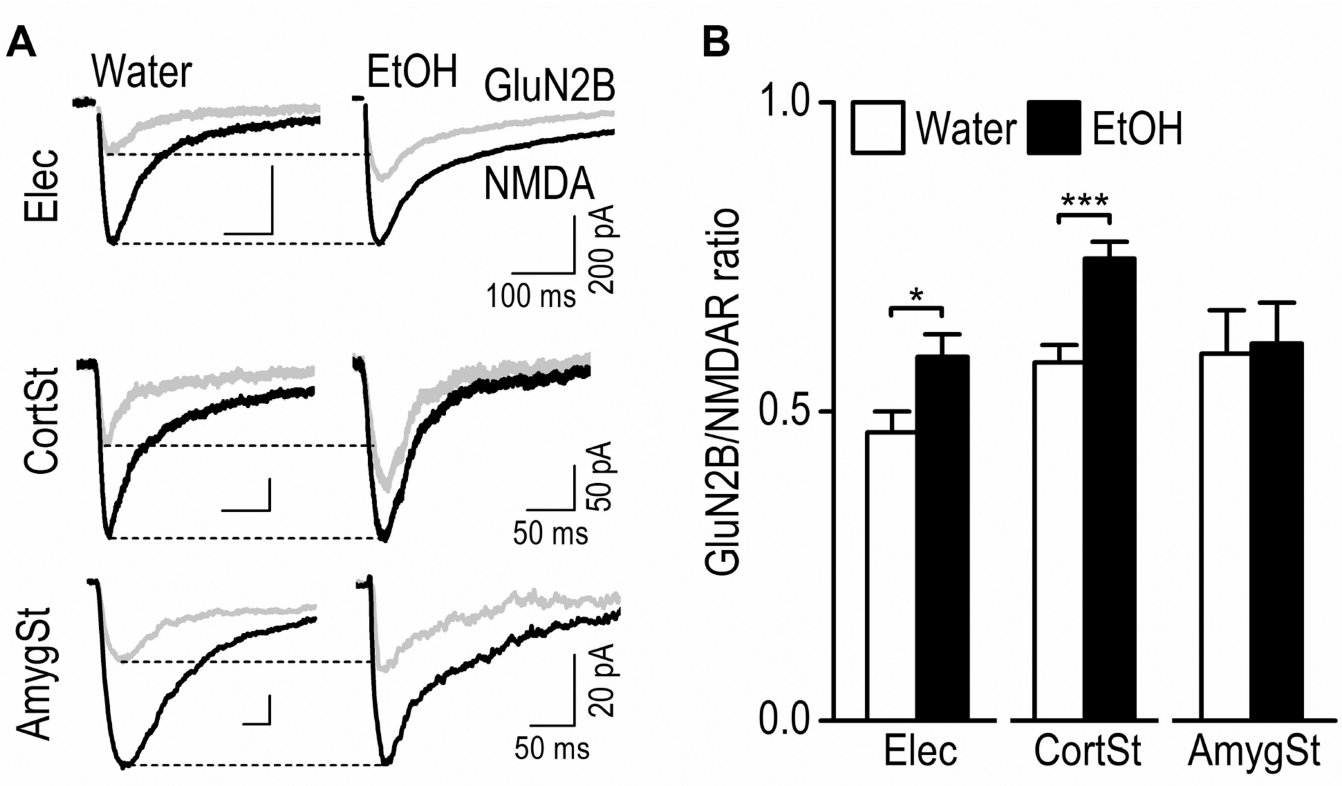

Fig. 4. Excessive alcohol intake potentiates the GluN2B/NMDAR ratio selectively at the mPFC afferents onto the rat DMS neurons

GluN2B-EPSCs were calculated by comparing the EPSCs generated in the present and absence of a GluN2B antagonist, Ro 25–6981 (0.5 μM). (A) Sample traces of NMDAR-EPSCs (black) and GluN2B–EPSCs (gray) in the DMS of alcohol (EtOH)-drinking rats and their water controls, evoked by electrical stimulation with the DMS (Elec, top), by optical stimulation of the CortSt input, (middle), or by optical stimulation of the AmygSt input, (bottom). (B) Bar graphs comparing the corresponding mean GluN2B/NMDA ratios in the indicated groups. Note that the GluN2B/NMDA ratio was greater for the CortSt input. *$p <$ 0.05, ***$p < 0.001$ by un-paired t test. n = 16 neurons from 10 rats for Water and 12 neurons from 9 rats for EtOH (Elec); 13 neurons from 8 rats for both groups (CortSt); 7 neurons from 5 rats for Water and 8 neurons from 7 rats for EtOH (AmygSt).

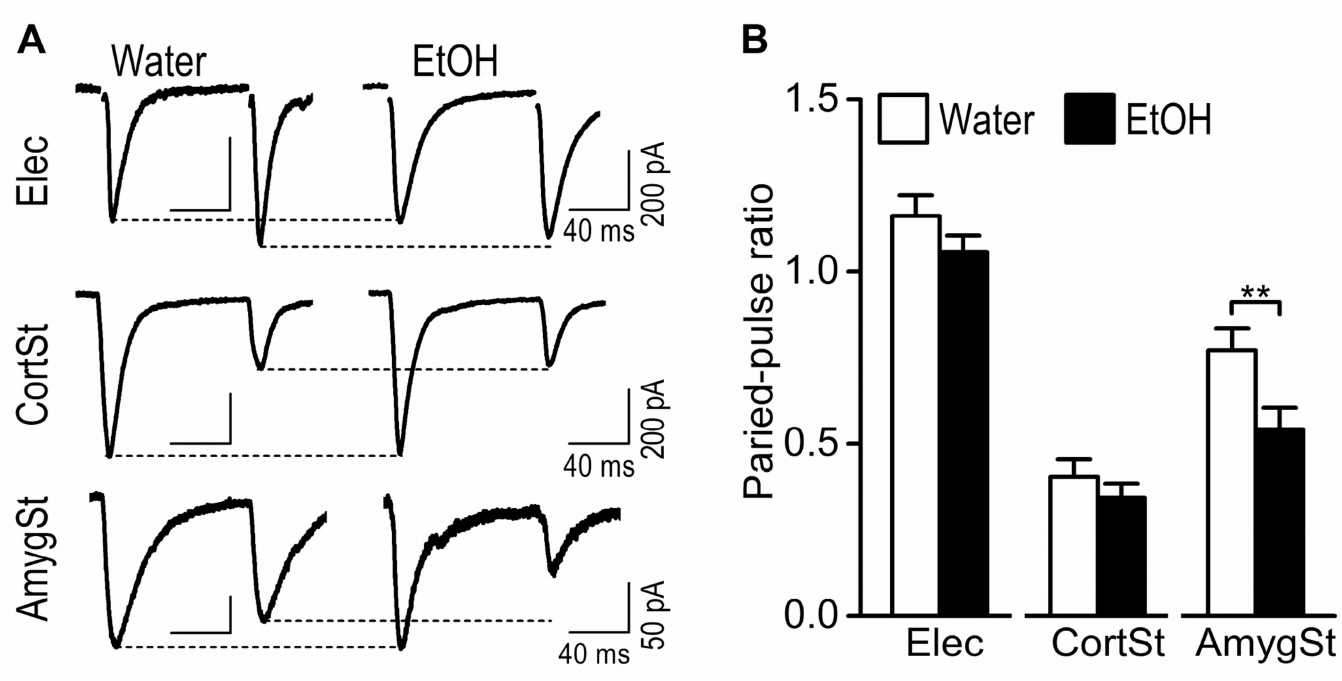

Fig. 5. Excessive alcohol intake reduces the paired-pulse ratio selectively at the BLA afferents to the DMS neurons

(A) Representative traces of paired-pulse AMPAR-EPSCs induced by electrical stimulation (top) or optical (middle) activation of the CortSt input in the alcohol and water groups. The bottom panel shows the EPSCs generated by optical stimulation of the AmygSt input. (B) Bar graph summarizing these paired-pulse ratios in the indicated study groups. $^{*}p < 0.05$ by un-paired *t* test. n = 22 neurons from 16 rats for Water and 22 neurons from 17 rats for EtOH (Elec); 18 neurons from 15 rats for Water and 14 neurons from 8 rats for EtOH (CortSt); 8 neurons from 6 rats for Water and 9 neurons from 9 rats for EtOH (AmygSt).

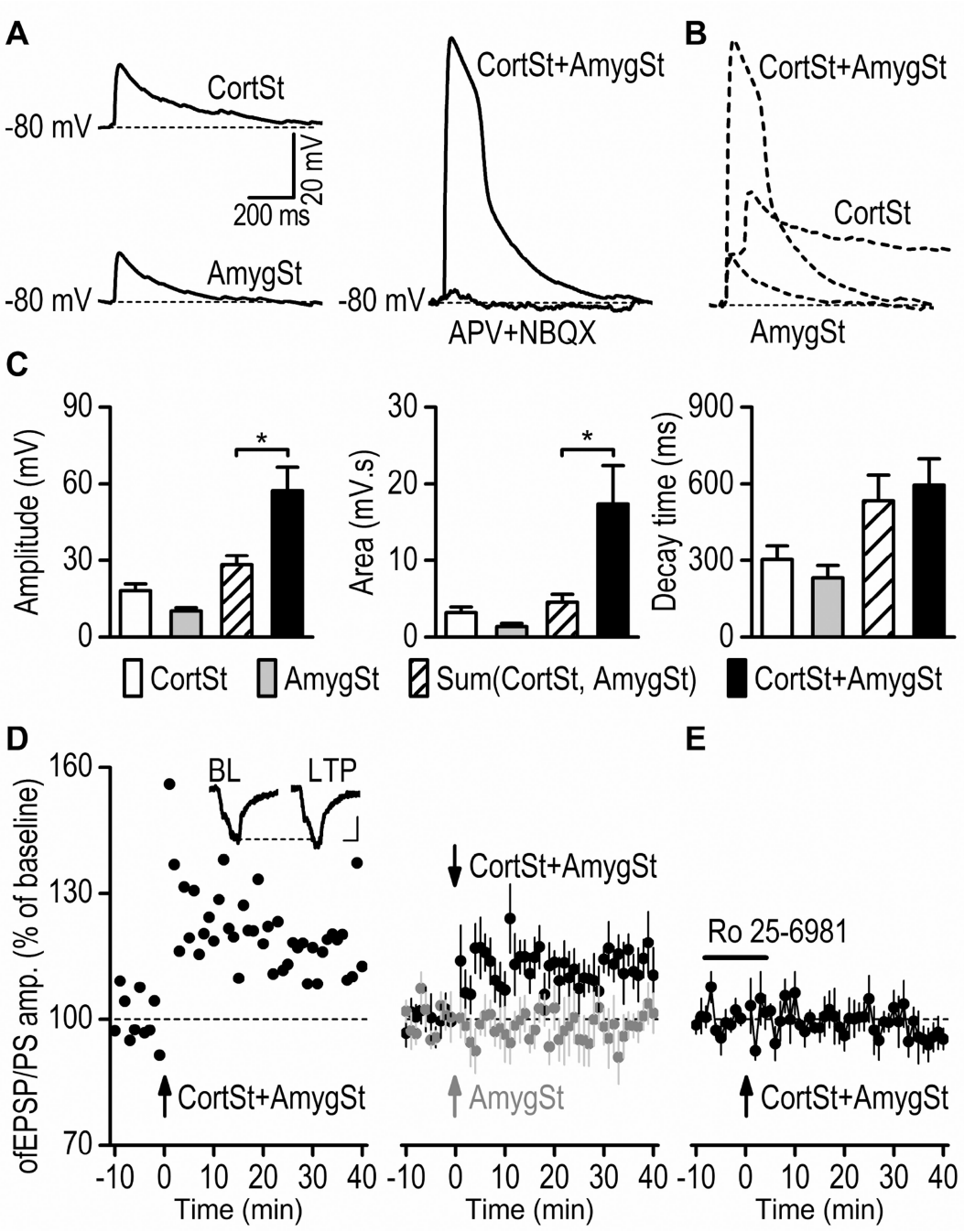

Fig. 6. Pairing of corticostriatal and amygdalostriatal inputs induces LTP in the rat DMS

(A) Sample traces of optogenetically-induced synaptic responses resulting from the individual activation of CortSt and AmygSt inputs (left) and from co-activation of both inputs (CortSt+AmygSt, right). Whole-cell current-clamp recording was used to measure membrane depolarization. Note that the membrane depolarization induced by co-activation of CortSt and AmygSt inputs were abolished by a cocktail of a NMDAR antagonist (APV, 50 μM) and AMPAR antagonist (NBQX, 10 μM). (B) Dashed traces (data from A) showing that co-activation induced a depolarization with a greater peak amplitude than the sum of the

individual peak amplitudes. (C) Bar graphs summarizing the amplitude of (left), the area under (middle), and the decay time (10–90% from the peak amplitude, right) of membrane-potential responses to light stimulation of CortSt, AmygSt, or both inputs. The calculated additive responses [sum(CortSt, AmygSt)] are added for comparison. Note that co-activation induced a membrane-potential response with a greater peak amplitude and area than the sum of the individual responses. $^{*}p < 0.05$, paired *t* test. n = 6 neurons from 6 rats. (D) Paired stimulation of the mPFC and BLA afferents at 50 Hz for 2 sec induced significant LTP in the rat DMS. Left, Representative recording showing long-term changes in the fEPSP/PS amplitude following the paired stimulation. The inset depicts the averaged 10-min response of the baseline (BL) and the averaged response 30–40 min after LTP induction (LTP). Scale bars: 5 ms, 50 mV. Right, Averaged responses before and after pairing CortSt and AmygSt stimulation (dark circles) or AmygSt stimulation only (gray circles). n = 8 slices from 4 rats (CortSt + AmygSt) and 6 slices from 3 rats (AmygSt only). (E) Bath application of Ro 25–6981 (5 μM) abolished the LT P induced by pairing CortSt and AmygSt inputs. The horizontal bar indicates the duration of Ro 25–6981 application. n = 5 slices from 5 rats.

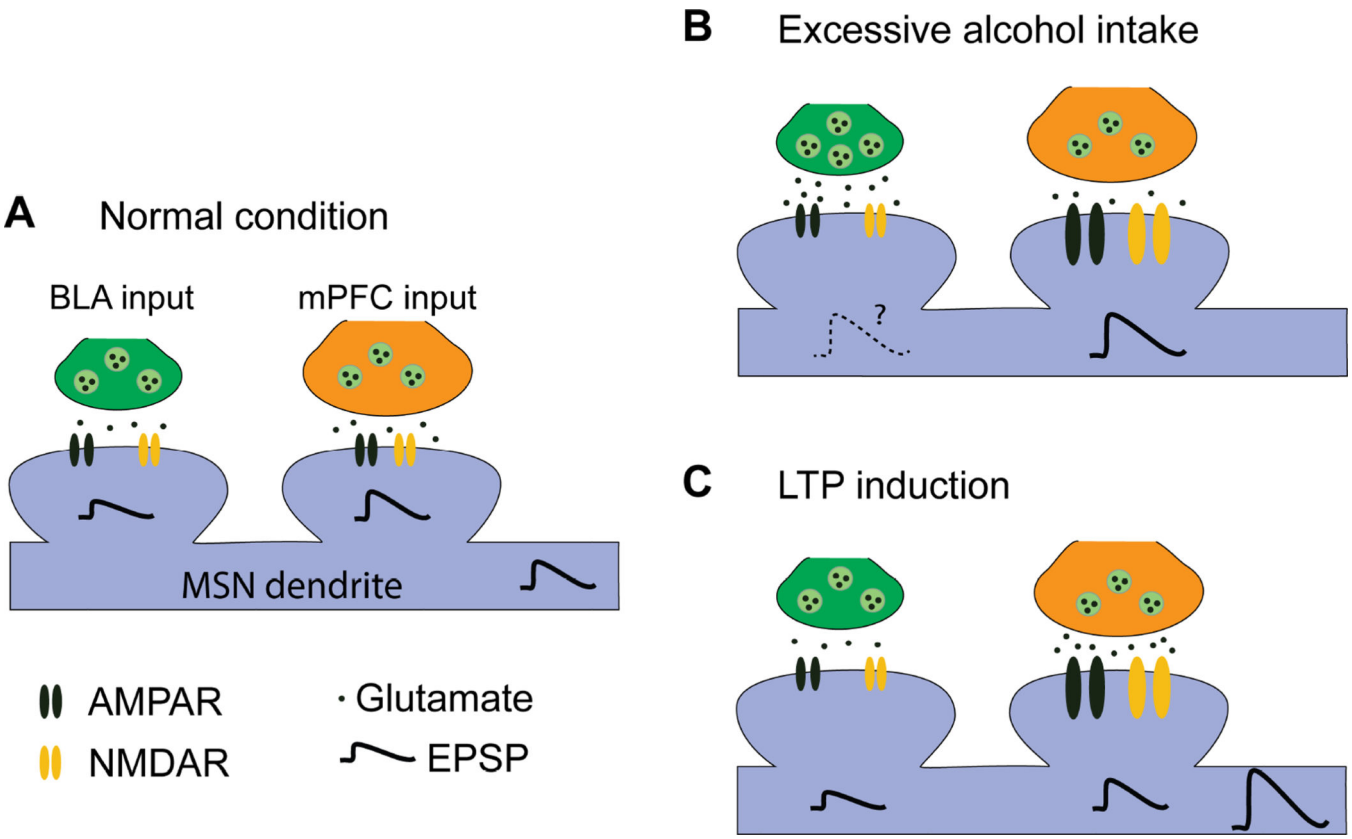

Fig. 7. Schematic illustrating the mPFC and BLA inputs to DMS MSNs and their responses to excessive alcohol intake and LTP induction

(A) In the normal condition, MSNs receive mPFC and BLA inputs with a great extent from the mPFC. (B) Excessive alcohol consumption potentiates AMPAR and NMDAR activities (as shown by the larger receptor size) at the mPFC input, as well as the probability of glutamate release at the BLA input. These changes cause enhancement of CortSt and possibly AmygSt transmission. (C) Paired stimulation of the mPFC and BLA inputs leads to large membrane depolarization and reliable LTP induction at the mPFC input.